Supplementary Materials

Enhanced capacitive energy storage of $NaNbO_3$-based relaxers via modulating phase structure strategy for high power energy storage

Jiangping Huang, Mingzhao Xu, Yue Pan, Yanchun Huang, Huanfu Zhou*, Xu Li*, Xiuli Chen*

Key Laboratory of New Processing Technology for Nonferrous Metal and Materials, Ministry of Education, Guangxi Key Laboratory of Optical and Electronic Materials and Devices, Guilin University of Technology, 541004, Guilin, China

* Corresponding authors.
E-mail address: zhouhuanfu@163.com (H. Zhou), lx100527@163.com (X. Li), cxlnwpu@163.com (X. Chen).

1. Experimental procedure and characterization of ceramics

The bulk ceramics $(1-x)NaNbO_3$-$xLa(Mg_{0.5}Zr_{0.5})O_3$ (expressed as LMZ100 x, with x = 0.06, 0.08, 0.10 and 0.12) were prepared by traditional solid-state sintering method. High-purity (> 99%) Na_2CO_3, Nb_2O_5, MgO, ZrO_2, and La_2O_3 powders were used as raw materials. After weighed by chemical stoichiometry, the raw materials were put into a nylon tank and ball-milled 5 hours using ZrO_2 balls and ethanol as the medium. Then drying at 100 ℃, the mixed powder is calcined at 850 ℃ with the heating rate of 5 °C/min and then ball-milled for 5 hours. The calcined powder is agglomerated with 8% polyvinyl alcohol (PVA) as a binding agent, and subsequently compacted into a circular disc measuring 8 mm in diameter and a thickness of 1.5 mm. Finally, the ceramic specimens sintered at temperatures ranging from 1180 - 1230℃ with the heating rate of 5 °C/min for 2 hours. During the sintering process, the samples were filled with powder of the same composition to reduce the volatilization of sodium and bismuth. To further investigate the energy storage properties, the sintered specimens were polished to a thickness of 0.1 ± 0.03 mm and coated with a silver paste of 2 mm in diameter. The temperature was increased to 700°C and then held for 30 minutes at a heating rate of 3°C. Oven and then held at a heating rate of 3°C per minute for 30 minutes to make a simple parallel plate capacitor for *P–E* loop tests. As the surface of the raw sintered specimens was very rough, the specimens were pre-polished, then ultrasonically cleaned, followed by PFM testing.

The phase structure and local structure evolution of all samples were characterized by X–ray powder diffraction (XRD, model X'Pert PRO; PA Nalytical, Almelo, The Netherlands) using Cu Kα radiation (λ = 0.15406 nm) and Raman spectrum, (XDR, Thermo Fisher Scientific, USA) tests, respectively. A scanning electron microscope (model GeminiSEM 300, OXIG, Oxfordshire, UK) was used to observe the microstructure of the specimens. The selected area electron diffraction (SAED) and TEM morphology were acquired by JEM–2100F. The dielectric-temperature spectrum of the ceramics was measured using a precision impedance analyzer (Model 4294A, Hewlett–Packard Co, Palo Alto, CA) in the temperature range of -160°C to 160°C and 520°C to 600°C with the heating rate of 2 °C/min. A simple parallel plate capacitor was fabricated for *P–E* loop testing (Ferroelectric Material Parameter Tester (RT66, Radiant Technologies, NM, USA)). Dielectric Charge Test System (CFD–003, TG Technologies, Shanghai, China) was used to measure

the charging/discharging properties. In order to investigate the domain structure, a piezoresponse force microscope (PFM, MFP-3D, UK) is applied by Pt/Ir-coated conductive tips (Nanosensors, Neuchatel, Switzerland) with an AC tip voltage of 3 V.

2. Results and Discussions

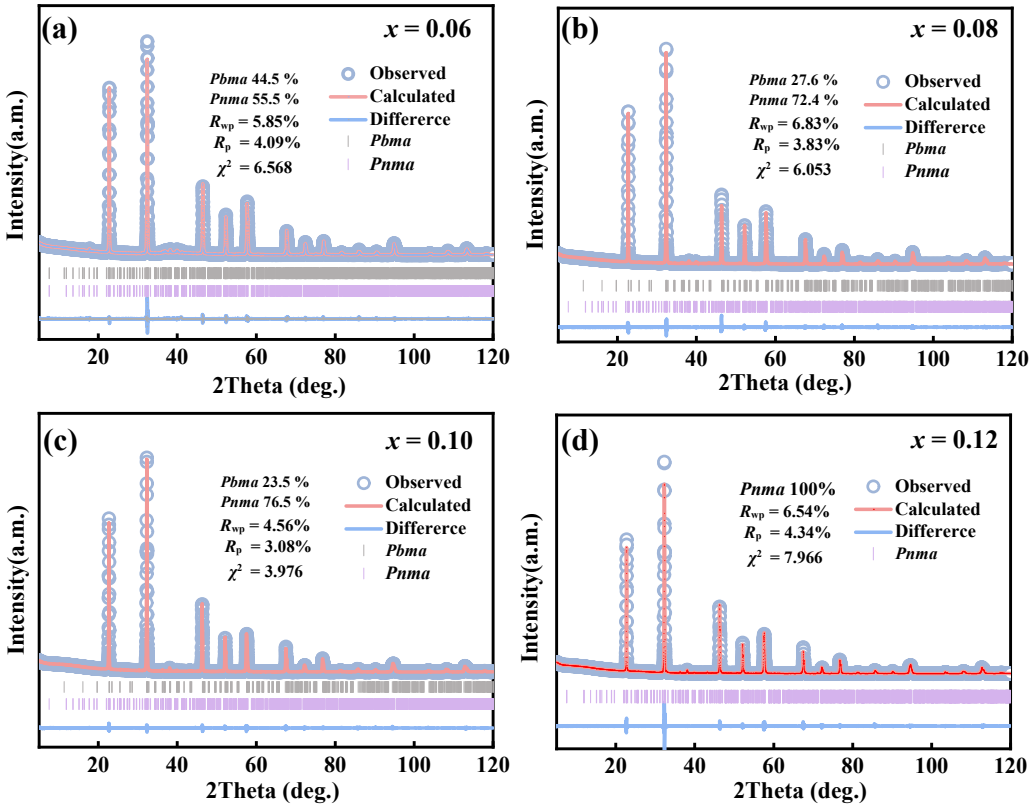

Fig. S1 (a)-(d) Refined XRD patterns of LMZ100*x* ceramic samples.

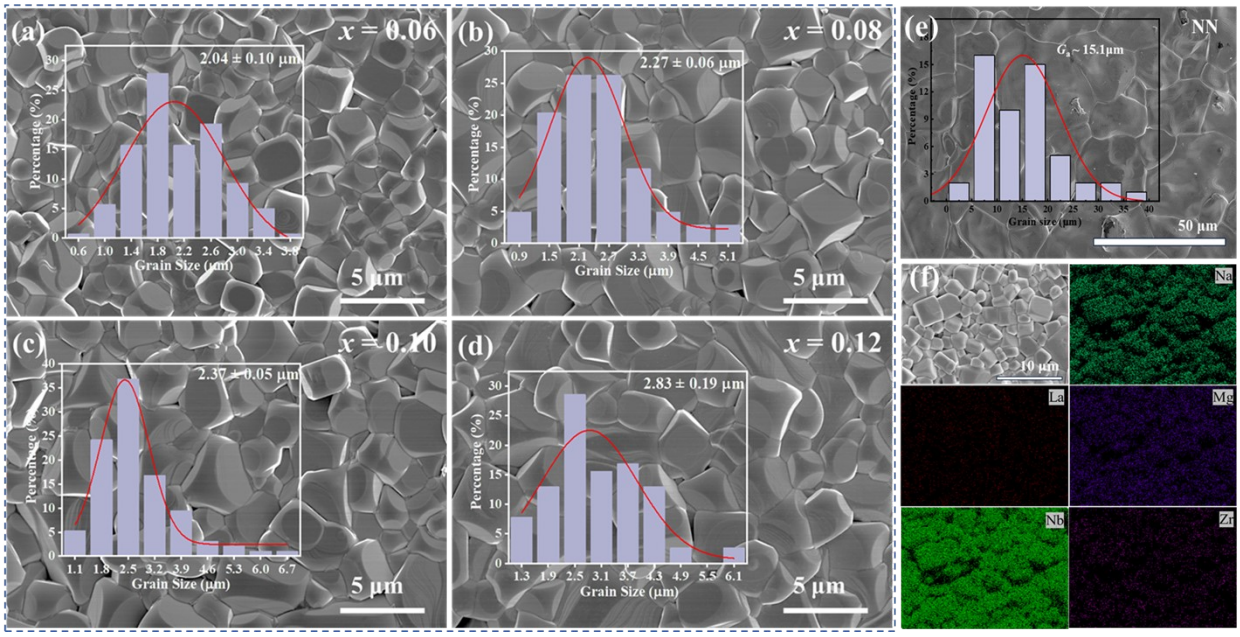

Fig. S2 (a)-(d) SEM images of LMZ100*x* ceramics and corresponding particle size distributions. (e) SEM image of pure NN ceramic (Illustration shows the grain size distribution of pure NN ceramic). (f) SEM images of LMZ10 ceramics and corresponding elemental distribution.

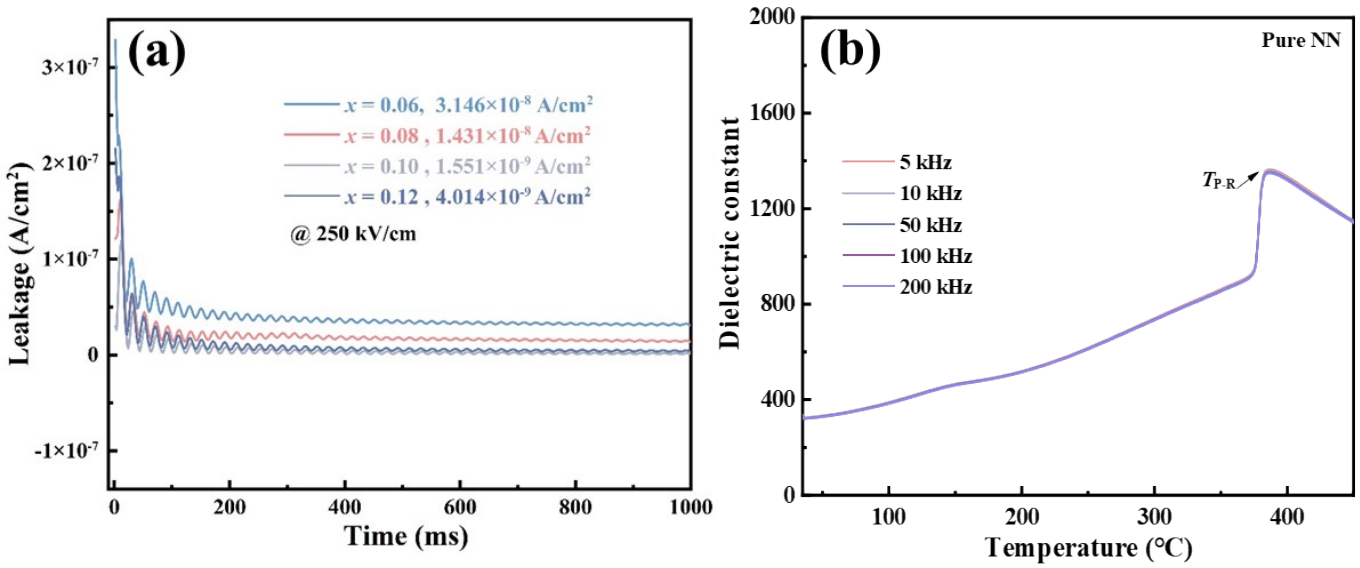

Fig. S3 (a) dielectric temperature spectrum of pure NN ceramic at various frequencies. (b) Leakage current density of LMZ100*x* ceramics at 250 kV/cm.

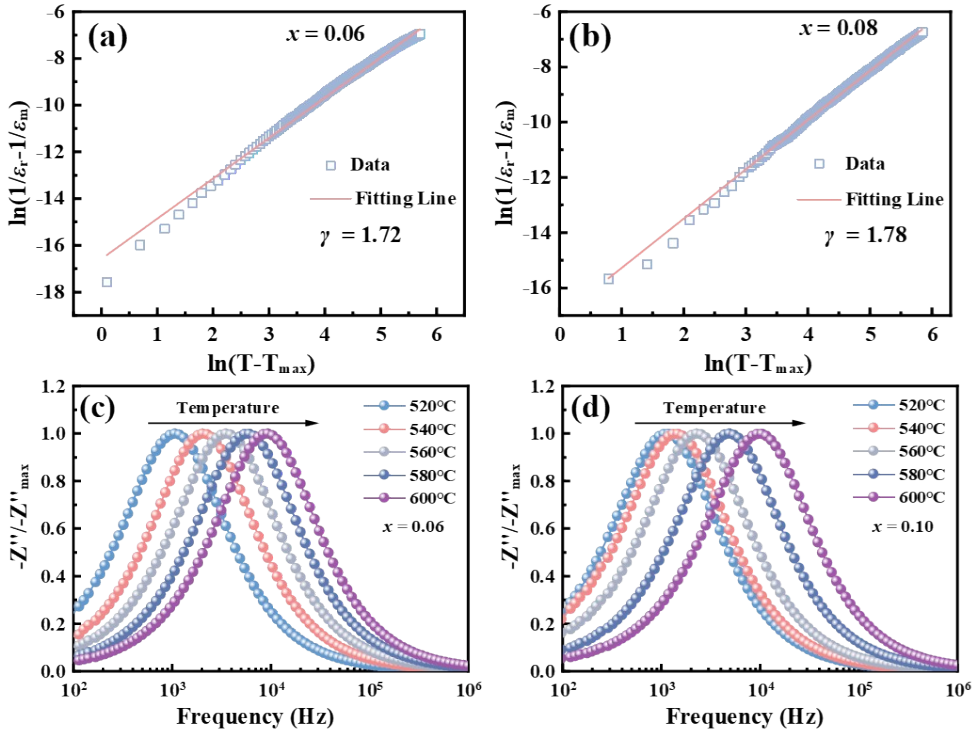

Fig. S4 (a-b) LMZ06 and LMZ08 ceramic components fitted dispersion factors according to the modified Curie-Weiss law. (c-d) LMZ06 and LMZ08 ceramics impedance normalized diagrams of the imaginary part.

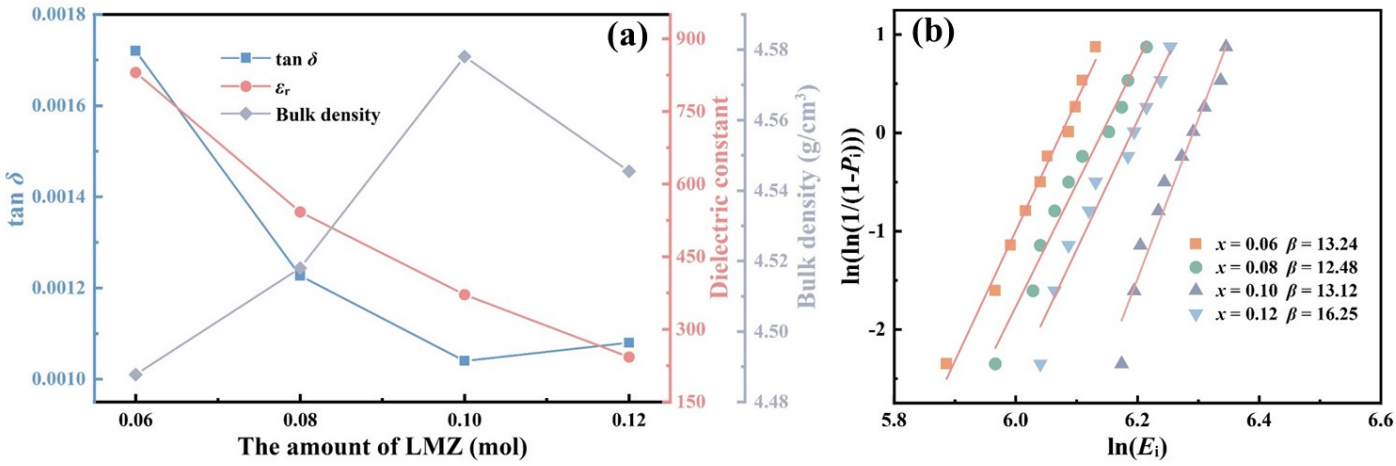

Fig. S5 (a) The variation of dielectric loss, dielectric constant and bulk density. (b) The Weibull distribution analysis of LMZ100*x* ceramics.